



ELSEVIER

Available online at www.sciencedirect.com

SCIENCE @ DIRECT®

Journal of Magnetism and Magnetic Materials 257 (2003) 87–94

Journal of
magnetism
and
magnetic
materials

www.elsevier.com/locate/jmmm

High field magnetic properties of $\text{Ag}_2\text{FeGeSe}_4$ in the temperature range 2–300 K

J.C. Woolley^a, G. Lamarche^a, A.-M. Lamarche^{a,*}, H. Rakoto^b, J.M. Broto^b,
M. Quintero^c, M. Morocoima^c, E. Quintero^c, J. Gonzalez^c, R. Tovar^c,
R. Cadenas^c, P. Bocoranda^c, J. Ruiz^c

^a Ottawa-Carleton Institute for Physics, University of Ottawa, 150 Louis Pasteur CP 450 SUCC A, Ottawa, Canada ON K1N 6N5,

^b LPMC-SNCMP INSA Complexe Scientifique de Rangueil, F31077 Toulouse Cedex 4, France

^c Departamento de Física, Facultad de Ciencias, Centro de Estudios de Semiconductores, Universidad de Los Andes, Merida 5101, Venezuela

Received 26 June 2002; received in revised form 19 August 2002

Abstract

Measurements of low field static magnetic susceptibility and of magnetization with pulsed magnetic fields up to 32 T have been made as a function of temperature on polycrystalline samples of the compound $\text{Ag}_2\text{FeGeSe}_4$ (AFG) which has an orthorhombic wurtz–stannite structure. The resulting data have been used to give information on the magnetic spin-flop (SF) and magnetic saturation transitions. It was found that AFG has a Néel temperature of 240 K, shows mainly antiferromagnetic behaviour with a very weak superimposed ferromagnetic component down to 60 K. At 60 K, a transition occurs resulting in an appreciably larger ferromagnetic effect below the transition. The ferromagnetic component is attributed to spin canting, with the transition at 60 K due to a discontinuous change in the canting angle. Thus, the SF and saturation fields show very different behaviour below and above 60 K. Details of the magnetic B – T phase diagrams were determined for the two phases and the results compared with the predictions of theoretical uniaxial models.

© 2002 Elsevier Science B.V. All rights reserved.

PACS: 75.25.+z; 75.50.–d

Keywords: Magnetic semiconductors; Spin-flop; Saturation; Wurtz–stannite structure; Spin canting

1. Introduction

As part of a research programme to investigate the magnetic properties of the quaternary magnetic

semiconductors, the magnetic behaviour of the compound $\text{Ag}_2\text{FeGeSe}_4$ (AFG) is being investigated. This compound has orthorhombic symmetry, with wurtz–stannite structure [1,2], and is basically anti-ferromagnetic (AF) [3]. The samples used in the present work are polycrystalline. Here, the variation of magnetic susceptibility (χ) with temperature and the magnetic behaviour at high magnetic fields for a number of temperatures have been determined.

*Corresponding author. Tel.: +1-613-562-5757; fax: +1-613-562-5190.

E-mail address: glamarch@science.uottawa.ca (A.-M. Lamarche).

Theoretical analysis e.g. [4,5] shows that for an AF material, in the magnetic field–temperature (B – T) plane of the magnetic phase diagram three phases can occur, the paramagnetic (P), the antiferromagnetic (AF) and the spin-flop (SF) phases. These analyses have been concerned mainly with uniaxial materials with an easy-axis z , and it is seen that the detail of the diagram depends on the orientation of the applied magnetic field with the z direction. Lines of interest in the diagram are the transitions between the phases, i.e. AF–SF, (B_f), the SF field, and AF–P and SF–P, (B_s), the saturation field. In the present work, measurements were made to investigate B_f and B_s in AFG at various temperatures.

2. Samples and measurements

The polycrystalline samples used were prepared by the melt and anneal technique [2], and X-ray powder diffraction photographs taken to check the conditions of the samples. Measurements of magnetic susceptibility χ as a function of temperature T in the range 2–300 K were made using a Quantum Design SQUID magnetometer with an external field of 1×10^{-2} T. Measurements of magnetization M as a function of applied field B were made: (i) over the temperature range 2–300 K, using the high field pulsed technique (Toulouse) [3] for fields up to 35 T and (ii) with a SQUID steady field system (Merida) up to 6 T.

3. Results and analysis

3.1. Magnetic susceptibility measurements

For the case of the magnetic susceptibility measurements, curves of χ vs. T are shown in Fig. 1 for $2 \text{ K} < T < 300 \text{ K}$, zero-field cooled (heating curve) and field cooled (cooling curve) data being shown. It is seen that in this temperature range two transitions occur, at 240 and 60 K. The form of the curves plus the analysis of the present experimental data (see below) indicates that the

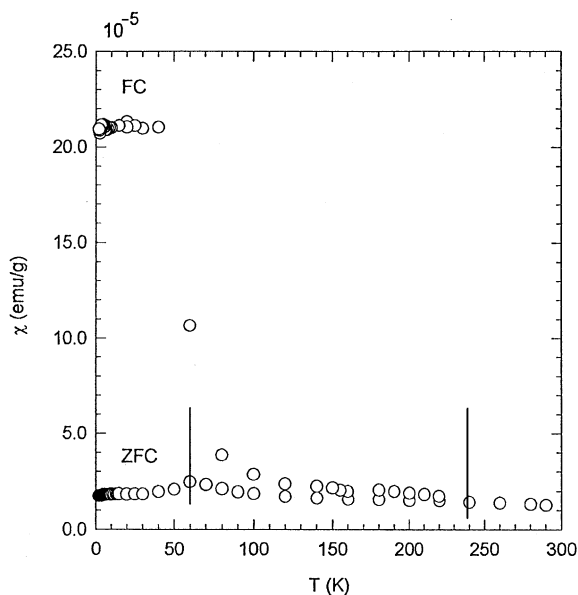


Fig. 1. Variation of magnetic susceptibility χ with temperature T for zero field cooled (ZFC) and field cooled (FC) conditions, determined by SQUID measurements with an applied field of 1×10^{-2} T. Vertical lines show transitions T_N and T_C .

higher transition is an AF type, with Néel temperature T_N of 240 K, but with a very weak ferromagnetic contribution superimposed. This type of transition has been observed previously in similar compounds [6] and can be attributed to crystallographic spin canting below T_N . At the lower transition T_C , the ferromagnetic contribution is found to increase appreciably, indicating an increase in the canting angle δ below T_C . Such behaviour is not unexpected in these quaternary materials, for, as shown by Dzialoshinsky and by Moriya [7], in structures of orthorhombic or lower symmetry, an anisotropic exchange interaction involving a combination of spin–orbit coupling and exchange interaction can result in spin canting when certain particular symmetry conditions are present. The space group symmetry ($\text{Pmn}2_1$) of AFG satisfies these conditions.

For convenience, in the present work, the three phases will be labelled phase P (paramagnetic), phase V (very weak ferromagnetic) and phase W (weak ferromagnetic). From the value of χ at low temperatures ($\sim 2 \times 10^{-5}$ emu/g), the angle of canting δ is seen to be very small, even for the

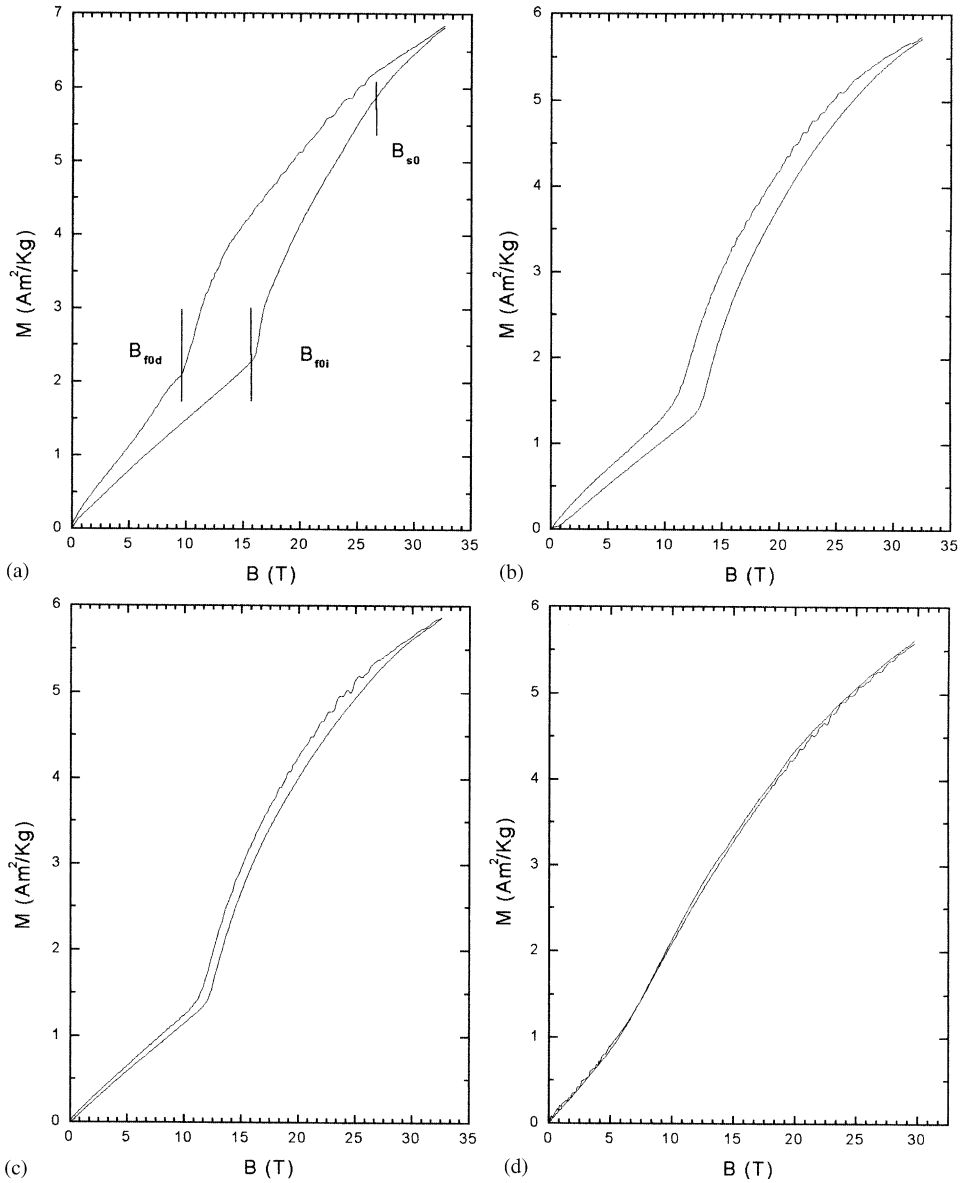


Fig. 2. Variation of magnetization M with applied magnetic field B for typical T values in the range $2\text{ K} < T < 60\text{ K}$, from pulsed field measurements: (a) 2 K, (b) 10 K, (c) 22 K and (d) 55 K. In (a), the vertical lines show the positions of the B_{f0i} , B_{f0d} , and B_{s0} points.

phase W. Because of the transition at 60 K, the Curie temperature T_f of the phase W cannot be directly observed, since the phase disappears before the Curie temperature is reached. However, extrapolation of the χ^2 vs. T data a little below 60 K gives an estimate of 70 K for the virtual value of T_f .

3.2. Pulsed field measurements on the weak ferromagnetic phase W

In the measurements of magnetization M using the pulsed field method, the variation of M with B was obtained at fixed temperatures in the range 2–300 K. Since the present work was done on

polycrystalline orthorhombic samples, the theory mentioned above cannot be expected to explain quantitatively the present data. However, it is useful in a qualitative discussion of the results.

Fig. 2 shows curves of M vs. B for the phase W, i.e. in the temperature range 2–60 K. In all of these curves, the SF B_f transition is clearly seen, and it is observed that an appreciable hysteresis effect is present. The theoretical analysis in Ref. [5] indicated that some hysteresis should occur, but it was not observed in that work on single crystal GdAlO_3 . For AFG, it is seen in Fig. 2 that at 2 K, with increasing B the AF–SF transition begins sharply at 16.3 T, while for decreasing B the corresponding point occurs at 9.5 T. Above these values, the M vs. B graphs show continuous curvature up to the highest value of B investigated, so that the sharp saturation point B_s usually observed with single crystal samples [8, Fig. 1] is not seen here. The M vs. B curves for other temperatures in this range show a similar form, but with the amount of hysteresis decreasing with increased temperature.

The form shown by these M vs. B curves is due to the polycrystalline nature of the orthorhombic sample, so that all possible values of θ , the angle between B , the applied field, and z , the direction of easy-magnetization, can be present in each sample. Theoretical analysis [9] shows that the SF transition is discontinuous at B_f when $\theta = 0$ but, as θ increases, becomes a smooth curve extending over a range of B that increases as θ increases, with M vs. B becoming a straight line at $\theta = 90^\circ$. It is also found [5] that the value of B_s varies with θ , B_s increasing as θ increases. On this basis, Fig. 3a shows a schematic diagram of typical forms to be expected for the M vs. B curves for different values of θ , while Fig. 3b shows the form to be expected from an appropriate summation over all values of θ . From these considerations, it is seen that the lowest B_f point observed in the M vs. B curve should correspond to the $\theta = 0$ condition, B_{f0} . For a sample showing an isotropic distribution of θ the relative number of crystallites with θ close to zero will be small. Hence, the sharp kink in the M vs. B curve at B_{f0} should not be very strong, and not as strong as the kinks shown in Figs. 2(a)–(c). However, AFG has the wurtz–stannite super-

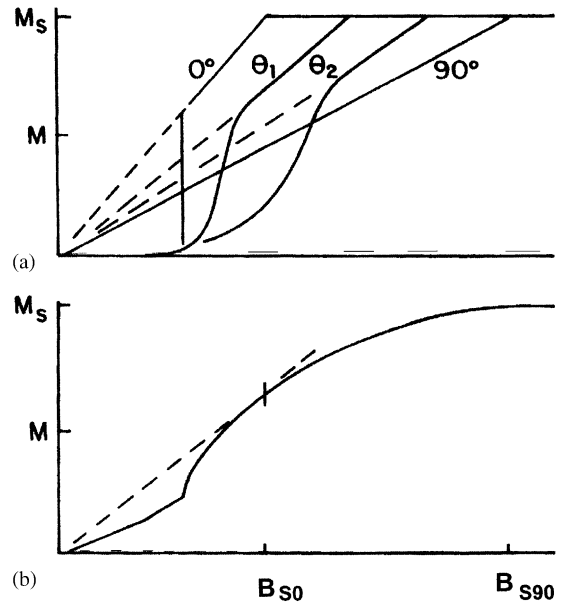


Fig. 3. (a) Schematic diagram to show the variation of magnetization M with applied field B for various values of θ , the angle between B and the easy-direction of magnetization z . (b) Expected variation of M with B obtained by summing over all values of θ occurring in a polycrystalline sample. B_{s0} and B_{s90} are the values of B_s for $\theta = 0^\circ$ and 90° , respectively.

structure based on hexagonal wurtzite, with a hexagonal close-packed anion structure. Hence, the fragmental components of the powdered sample can show mainly basal plane form, and hence considerably increase the $\theta = 0$ contribution to the observed magnetization in Figs. 2(a)–(c).

It is also seen from Fig. 3 that the tangent through the origin to the M vs. B curve gives an approximate estimate of the value of B_{s0} , the onset of the saturation transition. Thus a tangent through the origin to this curved part of the graph, as in Fig. 3b, gives an estimate of where the SF–P saturation transition starts to occur.

All the experimental curves given in Fig. 2 have a form similar to that shown in Fig. 3b. Thus, values of B_{f0} at the different temperatures are obtained for both increasing (B_{f0i}) and decreasing B (B_{f0d}), and these are shown in Fig. 4. Also, for the different temperatures, tangents through the origin gave values for B_{s0} and these also are shown in Fig. 4. Because of the overlap of the ranges of

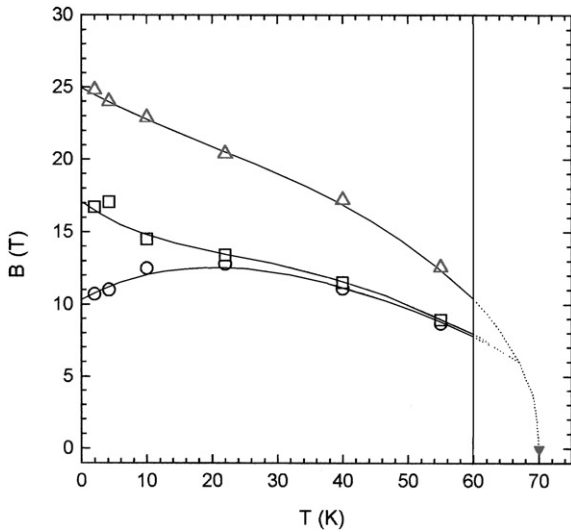


Fig. 4. Variation of B_{f0} and B_{s0} with temperature in the range $2\text{ K} < T < 60\text{ K}$. The B_{f0i} (\square), B_{f0d} (\circ) and B_{s0} (\triangle) values are obtained from the M vs. B curves of Fig. 2, and the Curie point (\blacktriangledown) from the magnetic susceptibility data. The dashed lines are extrapolations of the B_{s0} , B_{f0i} and B_{f0d} lines guided by the value of the Curie point.

the SF and saturation transitions, it is not possible to obtain from these data values of B_f and B_s other than those for $\theta = 0$, but it can be seen that B_{f90} exceeds B_{s0} , and B_{s90} is above 35 T, the upper limit of the experimental value of the applied field.

3.3. Pulsed field measurements on very weak ferromagnetic phase V

As seen above, the susceptibility data shows that a crystallographic spin transition occurs at 60 K, so that the results of measurements above this temperature correspond to the phase V. Typical curves for this case are shown in Fig. 5. It is seen that the effects of the magnetic transitions are smaller for this phase, the M vs. B graphs showing only small deviations from linearity. Each graph contains points from both ‘up’ and ‘down’ curves, so it is seen that no observable hysteresis occurs in this case. Also the size of the observed structures in the M vs. B graphs became smaller as the temperature was increased. In order to determine values of B_{f0} , various methods of treating the data

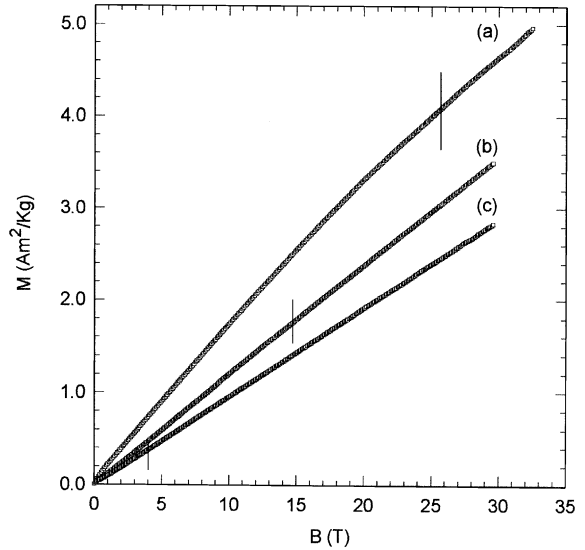


Fig. 5. Variation of magnetization M with applied magnetic field B for typical T values in the range $60\text{ K} < T < 240\text{ K}$, from pulsed field measurements. (a) 77 K, (b) 150 K and (c) 230 K. Vertical lines show B_{s0} transitions.

were used. Thus (a) the data were smoothed using the Savitzky–Golay filter method [10] and (b) derivative dM/dB curves were plotted. From the various curves thus obtained, approximate estimates of the values of B_{f0} could then be made, and these are shown in Fig. 6. It is seen that the values of B_{f0} in this phase are considerably larger than for phase W, the value of B_{f0} being $26 \pm 1\text{ T}$ at 77 K. This is discussed further below. Also, of course, no estimates of values of B_{s0} could be made.

3.4. Steady field measurements on the weak ferromagnetic phase W

As shown previously [6] for phase W in $\text{Ag}_2\text{FeSiSe}_4$ (AFS) at 4 K, the pulsed field and steady field measurements give different results. This is due to the presence of ferromagnetic domains in AFS, which have a relaxation time too long to follow the changes of the pulsed field B . Thus, the magnetic hysteresis effects due to the domains are observed only in the steady field measurements. In the case of AFS, these steady

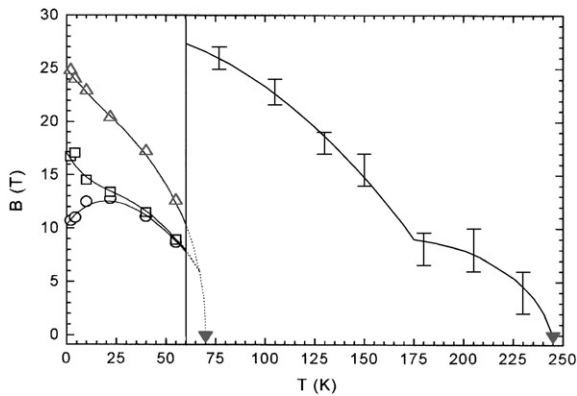


Fig. 6. Variation of B_{f0} and B_{s0} with temperature in the range $2\text{ K} < T < 245\text{ K}$. For the W phase (2 K to 60 K), the B_{f0i} (\square), B_{f0d} (\circ) and B_{s0} (\triangle) values are obtained from the M vs. B curves of Fig. 2, and the Curie point (\blacktriangledown) from the magnetic susceptibility data. The dashed lines are extrapolations of the B_{s0} , B_{f0i} and B_{f0d} lines guided by the value of the Curie point. For the V phase (60 K – 245 K), the $B_{f0}(I)$ values are obtained from the M vs. B curves of Fig. 5, and the Néel point (\blacktriangledown) from the magnetic susceptibility data.

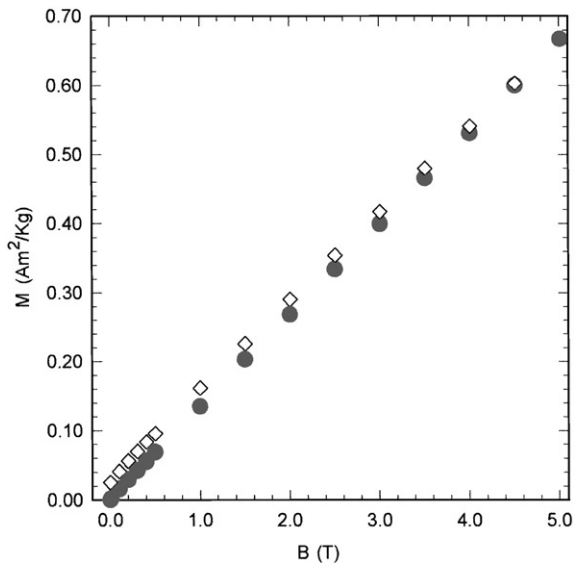


Fig. 7. Variation of magnetization M with applied magnetic field B at $T = 10\text{ K}$ from SQUID measurements. (\bullet) increasing field and (\diamond) decreasing field.

field data indicated that the canting angle δ was between 1° and 2° .

Steady field measurements were made at 4 K on an AFG sample and the resulting M vs. B curves

are shown in Fig. 7. It is seen that in this case, the data are similar to the pulsed field values in this range of B , but careful cyclic measurements indicated the presence of a small magnetic hysteresis. These results indicated that the canting angle δ in AFG is appreciably smaller than in AFS. From the values of remanence, it was estimated that δ for the W phase of AFG was of the order 0.05° , compared with $\sim 1.5^\circ$ for AFS. Since the value of δ for the V phase of AFG was still smaller, no attempt was made to estimate a value in this case.

4. Discussion

As indicated above, the difference in magnetic behaviour of the W and V phases of AFG is due to a change in the magnitude of the ferromagnetic component of the magnetization, that for the W phase being appreciably larger than that for the V phase. As was seen with AFS [6], this has a large effect on the relative values of B_f for the two phases. An approximate analysis of the AF SF behaviour [4] indicates that $B_f^2 = \{2\text{ K}/(\chi_2 - \chi_1)\}$, where χ_1 and χ_2 are the susceptibility with B parallel and perpendicular to z , respectively. If a canting of angle δ resulting in a small ferromagnetic component is added to the analysis, the modified relation becomes $B_f^2 = [2\text{ K}/\{(\chi_2 - \chi_1)\cos\delta + \chi_m \sin\delta\}]$ where χ_m is the effective ferromagnetic susceptibility. Since χ_m will be much larger than $(\chi_2 - \chi_1)$, even a small value of δ will result in a large reduction in B_f compared with the purely AF case. Thus, for AFS, B_{f0i} at 4.2 K was reduced to 0.4 T [6]. For the W phase of AFG, with a much smaller δ , at 4.2 K $B_{f0i} = 16.4\text{ T}$. For the V phase of AFG, values of B_{f0i} exist only above the transition temperature 60 K and, with δ appreciably smaller again, at $T = 77\text{ K}$ a value of $B_{f0i} = 26\text{ T}$ was obtained, indicating the appreciably larger value of B_f in this phase, as would be expected.

As indicated above, Fig. 6 shows the B – T phase diagram for the case of $\theta = 0$ (the easy-magnetization direction) for AFG. This divides into two parts at 60 K , corresponding to the W and V phases. Considering firstly the W phase,

here both the B_{f0} and the B_{s0} lines can be seen over the complete temperature range from 0 to 60 K. In the case of B_{f0} , there is appreciable hysteresis near 0 K which decreases as T is increased. The B_{f0i} and B_{f0d} curves should coalesce, together with the B_{s0} saturation curve, at the magnetic triple point (B_t , T_t), and beyond this point, the common curve should extend to the Néel point (0, T_N). As is seen in Fig. 6 a small amount of hysteresis is still present at 55 K and the B_{s0} curve is still appreciably higher than the B_{f0} curves, so that the triple point must occur above this temperature. However, this cannot be observed because of the phase change at 60 K. In Fig. 6, extrapolation of the B_{f0} and B_{s0} lines plus the use of a value of $T_N = 70$ K as given above, indicates a triple point T_{tF} at approximately (67 K, 6 T). Taking B_{f0} as the mean of B_{f0i} and B_{f0d} , it is seen that B_{f0} decreases linearly with increasing temperature, which is contrary to the form for a number of previously investigated compounds [5,11] for which B_{f0} increased with T . The hysteresis value $\Delta B_{f0}(= B_{f0i} - B_{f0d})$ also decreases with temperature and, writing ΔT for $T_t - T$, it is found that ΔB_{f0} varies as $(\Delta T)^5$.

In the case of the saturation transition, as seen in Fig. 6, the variation of B_{s0} with T shows the expected form and extrapolates to the triple point T_t . As indicated by Oliveira et al. [8], theoretical analysis gives the variation of B_{s0} with T as

$$B_{s0}(t) = B_{s0}(0)(1 - at^{3/2})$$

for $t \ll 1$, where $t = T/T_N$. Fig. 8 gives the experimental variation of B_{s0} with $T^{3/2}$ in the range $2 < T < 40$ K. Over this range, there is a deviation from linearity at $T = 2$ K. A similar result was observed by Oliviera et al. in the case of EuTe. From the slope of this line and using $T_N = 70$ K, in this case it was found that $a = 0.50$, while Oliveira's value for EuTe was 0.48.

Above 60 K, the data represent the phase diagram of the AF phase V. Here, values only for B_{f0} were obtained, and the variation of these with T are shown in Fig. 6. In contrast to the phase W, any hysteresis was too small to be observed. This again can be attributed to the presence of a stronger ferromagnetic component in the phase W, since this hysteresis effect has been observed only for the weak ferromagnetic phases

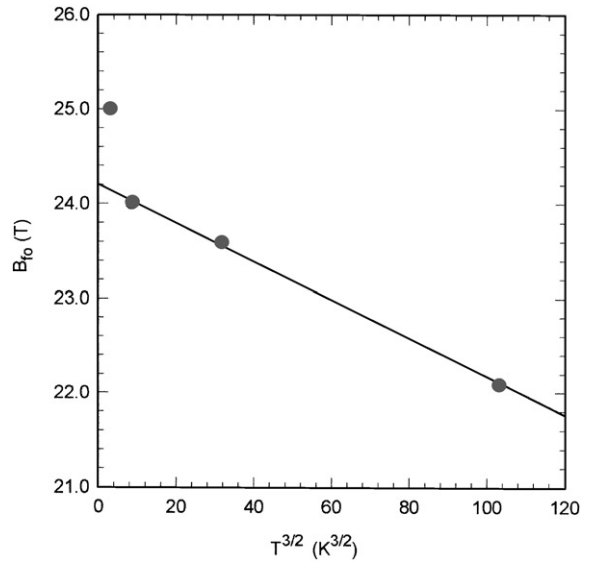


Fig. 8. Variation of B_{s0} with $T^{3/2}$, for $T \ll T_c$ in the phase W. The line is a linear fit to three points, as shown.

of the $Ag_2FeGeSe_4$, $Ag_2FeSiSe_4$ [6], Ag_2FeGeS_4 [12] and Ag_2FeSnS_4 [12] compounds. In Fig. 6, the values of B_{f0} extend to 240 K, the value of the Néel temperature determined from the susceptibility vs. temperature data (Fig. 1). The variation of B_{f0} with temperature was not accurately determined in this range, but the values are consistent with a postulated curve showing a triple point at approximately (175 K, 9 T) as shown in Fig. 6. More accurate $M-B$ data would be necessary to give a better estimate of this behaviour.

5. Conclusions

Because of a spin phase change at $T_c = 60$ K, the compound $Ag_2FeGeSe_4$ shows different magnetic behaviour above T_c (V phase) and below T_c (W phase), due to the difference in the ferromagnetic component in the two cases. As a result, the magnetic (B, T) phase diagram which indicates the values of the SF field B_f and the saturation field B_s is split into two very different parts. In the present work, the analysis of the M vs. B data at various temperatures was complicated by the polycrystalline condition of the samples, but it was shown

that each part of the phase diagram has the general form expected for these materials. An approximate theoretical analysis indicates that the SF field B_{FW} below T_c (W phase) should be appreciably smaller than the value B_{FV} above T_c (V phase), and this was found to be the case. The SF transition showed appreciable hysteresis for the W phase, but none was observed in the V phase. This hysteresis effect is attributed to the ferromagnetism of the phase concerned, the hysteresis effect not being observed in the V phase because its ferromagnetic component is small. With regard to the saturation field B_s , values could be determined only for the W phase, this transition occurring for the V phase at B values above the upper experimental limit.

Acknowledgements

The authors like to thank Dr. B. Raquet and Dr. L. D'Onofrio for stimulating discussions. Also, the authors are grateful to PCP (France)-CONICIT (Venezuela) and CDCHT-ULA for financial support.

References

- [1] W. Schafer, R. Nitsche, *Mater. Res. Bull.* 9 (1974) 645.
- [2] M. Quintero, A. Barreto, P. Grima, R. Tovar, E. Quintero, G. Sanchez Porras, J. Ruiz, J.C. Woolley, G. Lamarche, A.-M. Lamarche, *Mater. Res. Bull.* 34 (1999) 2263.
- [3] E. Quintero, R. Tovar, M. Quintero, J. Gonzalez, J.M. Broto, H. Rakoto, R. Barbaste, J.C. Woolley, G. Lamarche, A.-M. Lamarche, *J. Magn. Magn. Mater.* 210 (2000) 208.
- [4] Y. Shapira, S. Foner, *Phys. Rev. B* 1 (1970) 3083.
- [5] K.W. Blazey, H. Rohrer, R. Webster, *Phys. Rev. B* 4 (1971) 2287.
- [6] M. Quintero, R. Cadenas, R. Tovar, E. Quintero, J. Gonzalez, J. Ruiz, J.C. Woolley, G. Lamarche, A.-M. Lamarche, J.M. Broto, H. Rakoto, R. Barbaste, *Physica B* 294–295 (2001) 471.
- [7] I.E. Dzialoshinsky, *J. Phys. Chem. Solids* 4 (1958) 241; T. Moriya, *Phys. Rev. Lett.* 4 (1960) 228; T. Moriya, *Phys. Rev.* 120 (1960) 91.
- [8] N.F. Oliveira Jr., S. Foner, Y. Shapira, T.B. Reed, *Phys. Rev. B* 5 (1971) 2634.
- [9] S. Foner, *Magnetism I*, Academic Press, New York, 1963, p. 388.
- [10] A. Savitzky, M.J.E. Golay, *Anal. Chem.* 36 (1964) 1627.
- [11] Y. Shapira, S. Foner, *Phys. Rev. B* 1 (1970) 3083.
- [12] To be published by present authors.